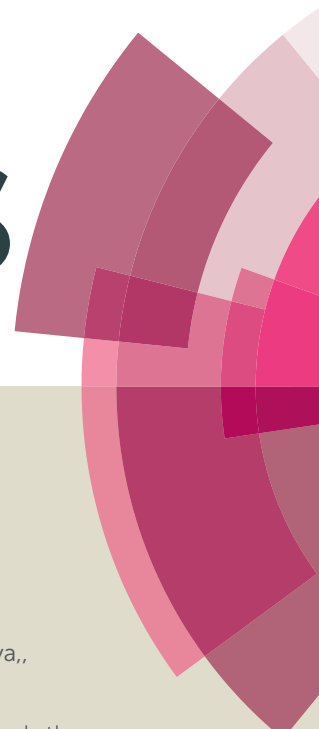


# RSC Advances



This article can be cited before page numbers have been issued, to do this please use: B. Bhattacharyya,, A. Kundu, A. Das, K. Dhara and N. Guchhait, *RSC Adv.*, 2016, DOI: 10.1039/C5RA19190D.



This is an *Accepted Manuscript*, which has been through the Royal Society of Chemistry peer review process and has been accepted for publication.

*Accepted Manuscripts* are published online shortly after acceptance, before technical editing, formatting and proof reading. Using this free service, authors can make their results available to the community, in citable form, before we publish the edited article. This *Accepted Manuscript* will be replaced by the edited, formatted and paginated article as soon as this is available.

You can find more information about *Accepted Manuscripts* in the [Information for Authors](#).

Please note that technical editing may introduce minor changes to the text and/or graphics, which may alter content. The journal's standard [Terms & Conditions](#) and the [Ethical guidelines](#) still apply. In no event shall the Royal Society of Chemistry be held responsible for any errors or omissions in this *Accepted Manuscript* or any consequences arising from the use of any information it contains.

# One-pot protocol for J-aggregated anthraimidazolediones catalyzed by phosphotungstic acid in PEG-400 under aerobic condition

Bhaswati Bhattacharyya,<sup>a</sup> Arijit Kundu,<sup>b</sup> Aniruddha Das,<sup>c</sup> Kaliprasanna Dhara\*<sup>c</sup> and Nikhil Guchhait<sup>c</sup>

<sup>a</sup>Department of Chemistry, A. P. C. Roy Govt. College, Darjeeling- 734010, India

<sup>b</sup>Department of Chemistry, Maulana Azad College, Kolkata-700013, India

<sup>c</sup>Department of Chemistry, University College of Science & Technology, University of Calcutta, 92, A.P.C. Road, Kolkata-700009, India.

*E-mail:* [chemkpd@gmail.com](mailto:chemkpd@gmail.com)

## Abstract:

A precise and productive one pot green protocol have been developed for the chemoselective synthesis of anthra[1,2-*d*]imidazole-6,11-diones using phosphotungstic acid (PTA) as a reusable catalyst on polyethylene glycol-400 (PEG-400) support under aerobic condition. It involves a simple synthetic procedure for a wide range of anthraimidazolediones from 1,2-diaminoanthraquinone and various aldehydes possessing  $\pi$ -enriched aromatic/heteroaromatic rings and lipophilic alkyl chains. In inert atmosphere, reaction followed a different pathway yielding a unique naphtho-quinoxaline derivative. Synthesized anthraimidazoledione derivatives had shown different self-aggregation morphologies influenced by the substitution pattern. A nice agreement between crystal packing pattern and photophysical properties with J-aggregation morphology were also observed. Representative derivatives exhibited contrasting fluorescence behaviors in transition from solution state to nanostructured solid state.

## Introduction

In the new era of research, low-dimensional self-aggregated organic materials (LMSOM) have gained much attention for their broad spectrum of electrical, magnetic and optical properties.<sup>1-4</sup> Performances of these organo-derived devices are correlated with the associative patterns present in their nanoarchitectures.<sup>5</sup> Therefore, designing of self-assembled structures with preferred shape and size by tailoring the structural features of the building blocks, i.e. modulating the  $\pi$ - $\pi$  stacking, hydrogen bonding and van der Waal's interactions etc., is the real challenge towards scientists.<sup>6</sup> Literature study revealed that some typical glycol-based chiral anthraimidazoledione derivatives had exhibited self-association properties.<sup>7</sup> Motivated by this observation we herein fabricated anthraimidazoledione scaffolds with a long lipophilic aliphatic chain or  $\pi$ -enriched aromatic/ heteroaromatic substituents at the 2-position of the imidazole ring which might find application in the field of organic nano-materials.

The regular synthetic methodology for imidazole derivatives is cyclocondensation-*cum*-oxidation (CCO) reaction between 1,2-diamino compounds with aldehydes.<sup>8</sup> However, 1,2-diaminoanthraquinone is exceptionally unreactive owing to the presence of an intramolecular hydrogen bond between N-H proton of the  $\text{-NH}_2$  group and the neighboring quinone  $\text{C}_9$ -carbonyl oxygen. Reported methodologies for the syntheses of anthraimidazolediones involved harsh reaction conditions *viz.* refluxing in ethanol in presence of  $\text{CF}_3\text{CO}_2\text{H}$ ,<sup>9</sup> or  $\text{Na}_2\text{S}_2\text{O}_5$  at  $130^\circ\text{C}$ ,<sup>10</sup> boiling in glacial  $\text{CH}_3\text{CO}_2\text{H}$  with sodium acetate,<sup>11a</sup> or with two equivalents of cupric acetate,<sup>11b</sup> in nitrobenzene at  $120$ - $140^\circ\text{C}$  for 8-24 hours,<sup>12</sup> in PEG-400 at  $120^\circ\text{C}$  for 18 hours<sup>13</sup> and a two step process which required refluxing overnight with formic acid in ethanol followed by in situ oxidation with lead tetraacetate in acetic acid.<sup>14</sup> Huang and Lin *et. al.*<sup>15</sup> and Maity *et. al.*<sup>7</sup> had achieved syntheses of certain types of anthraimidazoledione derivatives at room temperature

using concentrated sulphuric acid in DMF and a combo catalyst  $\text{VO}(\text{acac})_2$  -  $\text{Ti}(\text{OBu})_4$  -  $\text{CeCl}_3$  with molecular  $\text{O}_2$  as oxidant, respectively. It is pertinent to mention here that several of these methodologies were explored with some selected substrates only. So the search for an easier general protocol with environmentally benign catalytic system for the preparation of anthraimidazoledione derivatives was the major thrust of our work.

Commercially available heteropolyacids (HPAs) is very much significant for their “value adding properties”.<sup>16</sup> HPAs with their Keggin structure, manifest very high Brönsted acidic character comparable to super-acids and show unique redox properties under aerobic condition.<sup>16</sup> Of them, phosphotungstic acid (PTA) and phosphomolybdic acid (PMA) are already in use for several types of organic transformations.<sup>17-21</sup> In this methodology preference was given to PTA over PMA for its higher acidity and greater thermal stability.<sup>22</sup>

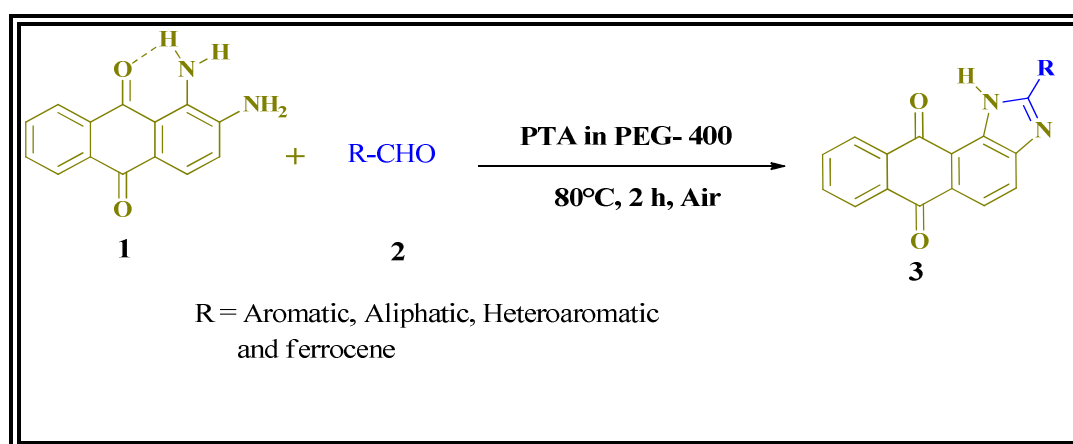
The difficulties with solid HPAs as heterogeneous catalysts are their inherent nature to absorb polar and especially basic compounds by forming a “pseudoliquid” phase.<sup>23</sup> The extent of absorption of those molecules depend on their molecular sizes.<sup>23</sup> Additionally the compounds bearing alcoholic functionality are easily desorbed from HPAs whereas, for the basic amino compounds, elevated temperature is required for desorption.<sup>23</sup> So, to maintain the virtues of hydroxylic environment and to avoid the “pseudoliquid” formation, poly(ethylene glycol) (PEG-400) was chosen as a medium because of its high thermal stability (up to 150-250°C) towards oxidative environment of HPAs.<sup>24</sup> PEGs are also known to act as phase-transfer catalyst since they possess both hydrophobic crown ether framework along with polar hydroxyl groups. These substances are cheap, easily available, biodegradable and may stand in comparison to other recently much publicized media like micellar systems or costly ionic liquids.<sup>25</sup>

Considering the above facts we have used PTA as solid heterogeneous catalyst on PEG-400 support to prepare anthra[1,2-*d*]imidazole-6,11-dione derivatives in presence of air. A comparative study was performed with the crystal structure, morphology and photo-physical property to correlate the substituent effect of the anthraimidazoledione derivatives.

## Results and discussion

In the hunt for optimum reaction condition we carried out extensive screening tests employing a representative reaction between 1,2-diaminoanthraquinone (**1**) (1 mmol) and *p*-chlorobenzaldehyde (**2c**) (1 mmol) to furnish the product **3c** (**Scheme 1**) in presence of different oxidants and acid catalysts. The other parameters such as solvent, temperature and reaction time etc. were also varied and the results have been summarized in Table 1. It is evident from Table 1 that the oxidant ammonium persulfate [ (NH<sub>4</sub>)<sub>2</sub>S<sub>2</sub>O<sub>8</sub> ] in ethanol solvent, used successfully for the synthesis of benzimidazoles,<sup>26</sup> had negligible efficacy in this specific case even after 10 hours (Table 1, entry 1). *N*-iodosuccinimide (NIS) in acetonitrile (Table 1, entries 2 and 3), which was initially employed in our laboratory for simple CCO type reaction at room temperature with good yield,<sup>27</sup> led to moderate yield of **3c** even at 60 °C. Both L-proline, as an organocatalyst in ethanol and polyphosphoric acid in dichloromethane with its dual nature as acid and dehydrating agent (Table 1, entries 4 and 5) failed to prove as suitable reagents after six and ten hours respectively. At this stage we turned our attention towards HPAs as more proficient catalytic system. We had chosen phosphotungstic acid (PTA) in dichloromethane at room temperature which increased the yield of **3c** (35%) a bit though the reaction was slow and incomplete even after 20 h (Table 1, entry 6). But, employing PMA as catalyst in similar solvent system diminished the yield of **3c** to

20% (Table 1, entry 7). It may be mentioned here that the general limitations of HPAs as solid heterogeneous catalysts are their low specific surface area (approx.  $5 \text{ m}^2 \text{ g}^{-1}$ ).<sup>23</sup> To overcome this predicament, we had dispersed PTA on solid surface such as silica gel to obtain better surface catalytic activity (Table 1, entries 8 and 9) but no significant change in the yield of the product was obtained. This phenomenon could be interpreted as the loss of Keggin structure due to interaction between the surface silanol groups of silica and surface P atoms of PTA.<sup>23</sup> Since HPAs absorb polar molecules which affect the yields of the corresponding products, we had explored the effects of polar protic and polar aprotic solvents to raise the yield of the products. It provided yields of the product in the order 55%, 60%, 63% and 70% in ethanol, acetonitrile, dimethylformamide and PEG-400 respectively (Table 1, entries 10, 11, 12 and 13). So PEG-400 was favored for its better activity as supportive medium. Henceforth, additional screening tests were performed with PTA in PEG-400 in order to find out the best reaction condition by varying temperature and time (Table 1, entries 14, 15, 16, 17 and 18). Finally the optimum condition was achieved with the reaction being carried out at  $80^\circ\text{C}$  for 2 hours by using PTA (10 mole %) in PEG-400 (3 ml) when 85% yield of the desired product (Table 1, entry 16) was obtained.



**Scheme 1:** Chemoselective CCO protocol for the synthesis of anthraimidazoledione derivatives

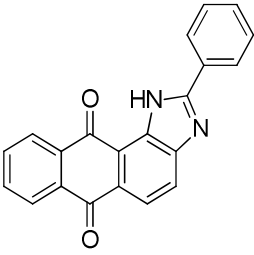
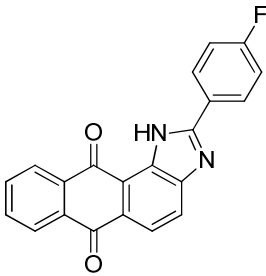
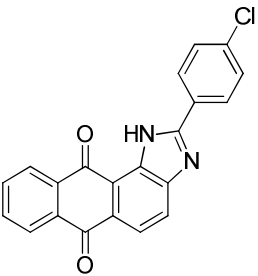
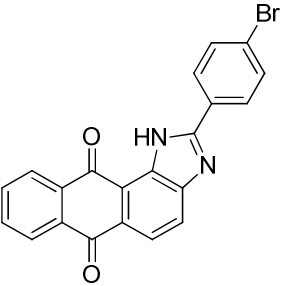
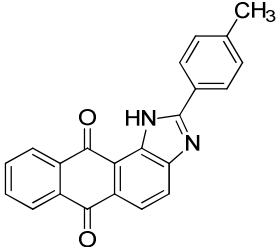
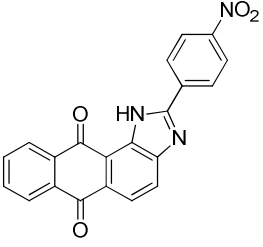
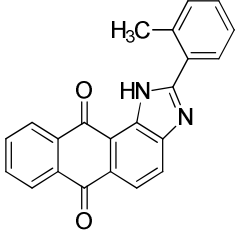
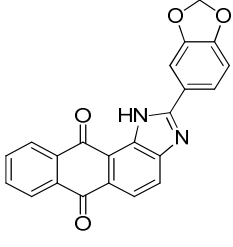
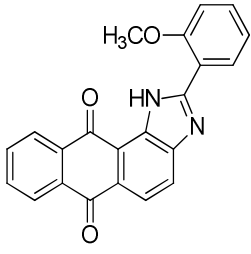
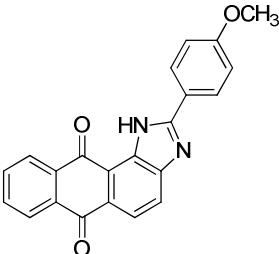
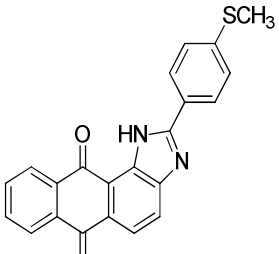
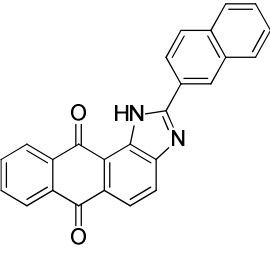
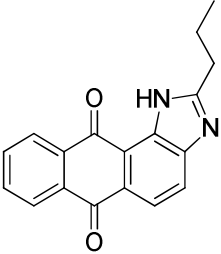
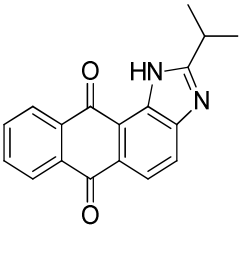
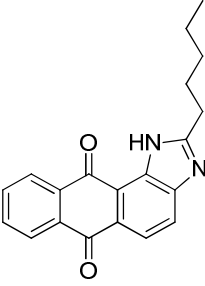
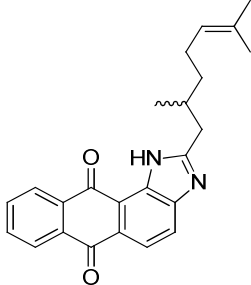
**Table 1.** Optimization study using **1** with aldehyde **2c**<sup>a</sup>

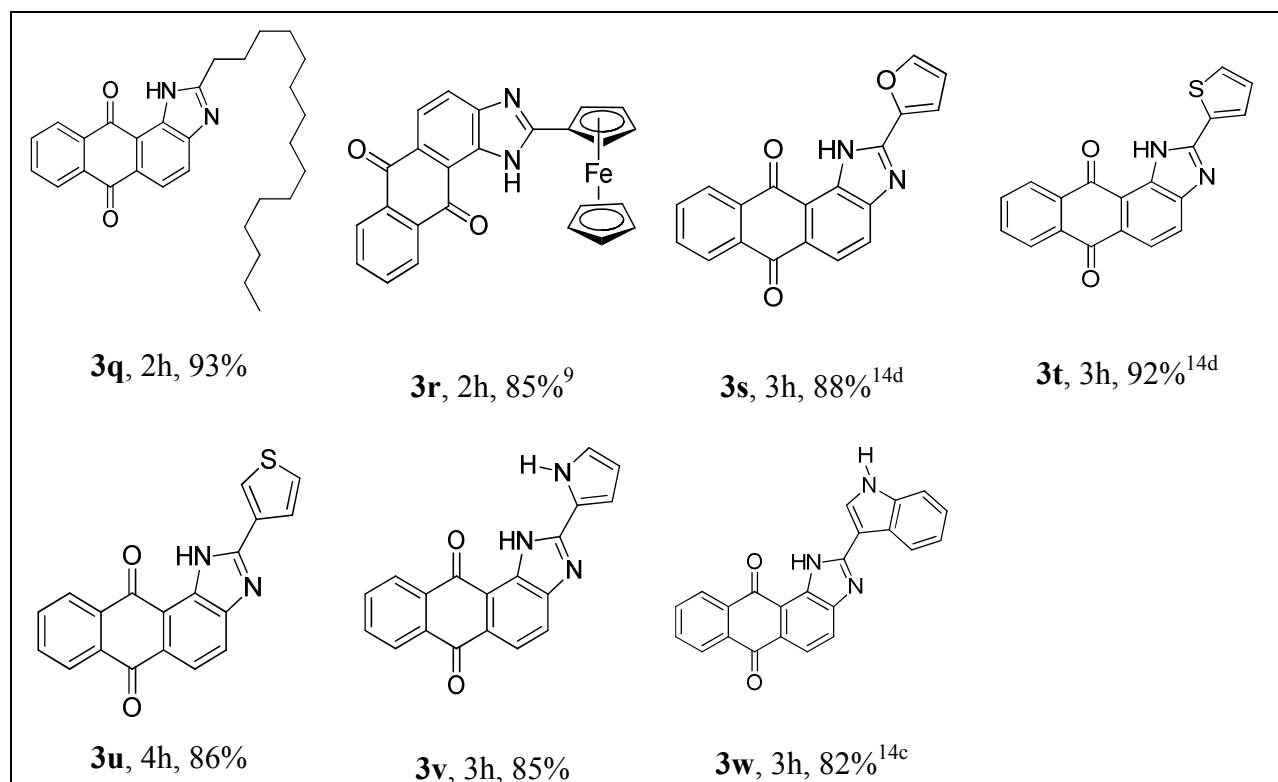
Sl. No.	Oxidant/catalyst	Conditions	Time	Temp	Yield <sup>b</sup> (%)
1	(NH <sub>4</sub> ) <sub>2</sub> S <sub>2</sub> O <sub>8</sub> (1.1 mmol)	EtOH	10 h	r. t.	0
2	NIS (1.2 mmol)	ACN	4 h	r. t.	22
3	NIS (1.2 mmol)	ACN	6 h	60 °C	32
4	L-Proline (30 mol %)	EtOH	6 h	60 °C	15
5	Polyphosphoric acid (10 mol %)	CH <sub>2</sub> Cl <sub>2</sub>	10 h	r.t.	10
6	Phosphotungstic acid (10 mol %)	CH <sub>2</sub> Cl <sub>2</sub>	20 h	r.t.	35
7	Phosphomolybdic acid (10 mol %)	CH <sub>2</sub> Cl <sub>2</sub>	20 h	r.t.	20
8	Phosphotungstic acid-SiO <sub>2</sub>	ACN	10 h	r.t.	10
9	Phosphotungstic acid-SiO <sub>2</sub>	ACN	6 h	reflux	20
10	Phosphotungstic acid (10 mol %)	EtOH	6 h	reflux	55
11	Phosphotungstic acid (10 mol %)	ACN	6 h	reflux	60
12	Phosphotungstic acid (10 mol %)	DMF	6 h	60 °C	63
13	Phosphotungstic acid (10 mol %)	PEG-400	6 h	50 °C	70
14	Phosphotungstic acid (20 mol %)	PEG-400	6 h	50 °C	75
15	Phosphotungstic acid (10 mol %)	PEG-400	3 h	70 °C	80
<b>16</b>	<b>Phosphotungstic acid (10 mol %)</b>	<b>PEG-400</b>	<b>2 h</b>	<b>80 °C</b>	<b>85</b>
17	Phosphotungstic acid (10 mol %)	PEG-400	2 h	100 °C	85
18	Phosphotungstic acid (10 mol %)	PEG-400	3 h	80 °C	85

<sup>a</sup> Reaction: aldehyde (1 mmol), 1,2-diaminoanthraquinone (1 mmol)<sup>b</sup> Isolated and optimised yield, r.t.= room temperature

To study the extent and limitations of this CCO protocol we explored the new methodology with variety of aldehydes possessing  $\pi$ -enriched aromatic/heteroaromatic rings and lipophilic alkyl chains reacting with 1,2-diaminoanthraquinone **1** (Scheme 1, Table 2). In all cases reaction progressed smoothly with good to excellent yields of the products. The reactions were consistently executed at the 1 mmol scale and no change of the product yield was observed when scaled up to the 10 mmol. High chemoselectivity was a rewarding aspect of this CCO protocol as no undesired 1,2-disubstituted derivative was obtained. It was pertinent to mention here that among the three types of aldehydes used, in terms of reaction times and isolated yields, aliphatic aldehydes with a chain length of C<sub>4</sub>-C<sub>16</sub> (**2m-2q**, Table 2) showed highest reactivity followed by heteroaromatic aldehydes (**2s-2w**, Table 2) and then aromatic aldehydes (**2a-2l**, Table 2). Metallocenealdehyde like ferrocene carboxaldehyde, **2r** was equally reactive and yielded 85% of **3r** (Table 2) within 2 hours. All the new products were well characterized by spectral (IR, <sup>1</sup>H and <sup>13</sup>C NMR) and elemental analyses. The known products were identified by comparing the literature reports with their respective <sup>1</sup>H-NMR spectra and melting points.

**Table 2.** PTA in PEG-400 catalyzed synthesis of anthra[1,2-*d*]imidazole-6,11-diones<sup>a</sup>

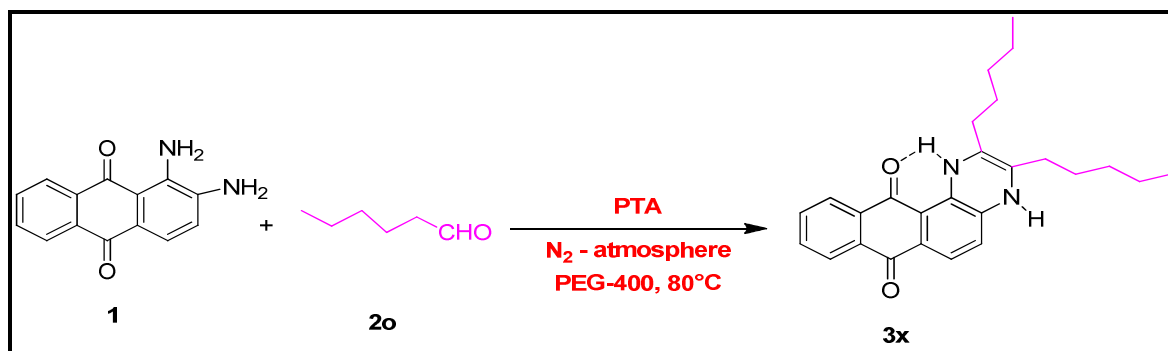
 <b>3a</b> , 2h, 87% <sup>15</sup>	 <b>3b</b> , 2h, 83% <sup>11b</sup>	 <b>3c</b> , 2h, 85% <sup>15</sup>	 <b>3d</b> , 3h, 75% <sup>15</sup>
 <b>3e</b> , 4h, 82% <sup>11b</sup>	 <b>3f</b> , 5h, 60% <sup>15</sup>	 <b>3g</b> , 3h, 77% <sup>11b</sup>	 <b>3h</b> , 3h, 75% <sup>15</sup>
 <b>3i</b> , 4h, 70% <sup>13</sup>	 <b>3j</b> , 3h, 80% <sup>44</sup>	 <b>3k</b> , 3h, 82%	 <b>3l</b> , 4h, 80% <sup>10</sup>
 <b>3m</b> , 1.5h, 96% <sup>15</sup>	 <b>3n</b> , 1.5h, 92% <sup>15</sup>	 <b>3o</b> , 1h, 97%	 <b>3p</b> , 1.5h, 90%



<sup>a</sup> Reactions: aldehyde (1 mmol), 1,2-diaminoanthraquinone (1 mmol); PTA (10 mol %); Solvent PEG 400; 80 °C.

In order to comprehend the reaction pathway for the formation of anthraimidazolidione derivatives involving PTA and PEG-400, an experimental strategy was developed with aldehyde **2o** since **3o** was formed within a short period of time. A mixture of **2o** and **1** was stirred in PEG-400 at 80 °C for 45 minutes in absence of PTA and then quenched with water and worked up. Compound **1** was returned back in almost quantitative amount without isolation of imine or cyclo-condensed product. In a successive experiment, PTA (10 mol %) was added to the reaction mixture after 45 minutes and the reaction was complete in next 1 hour with the formation of the product, **3o**. This result demonstrated the importance of both PTA and PEG-400 for cyclocondensation step which involved the aldehydic functional group of **2o** with amino groups of **1**. PEG-400 formed strong inter-molecular H-bonds with its free hydroxyl groups and C9-carbonyl oxygen of **1** thus reducing the strength of intra-molecular H-bond existing in compound

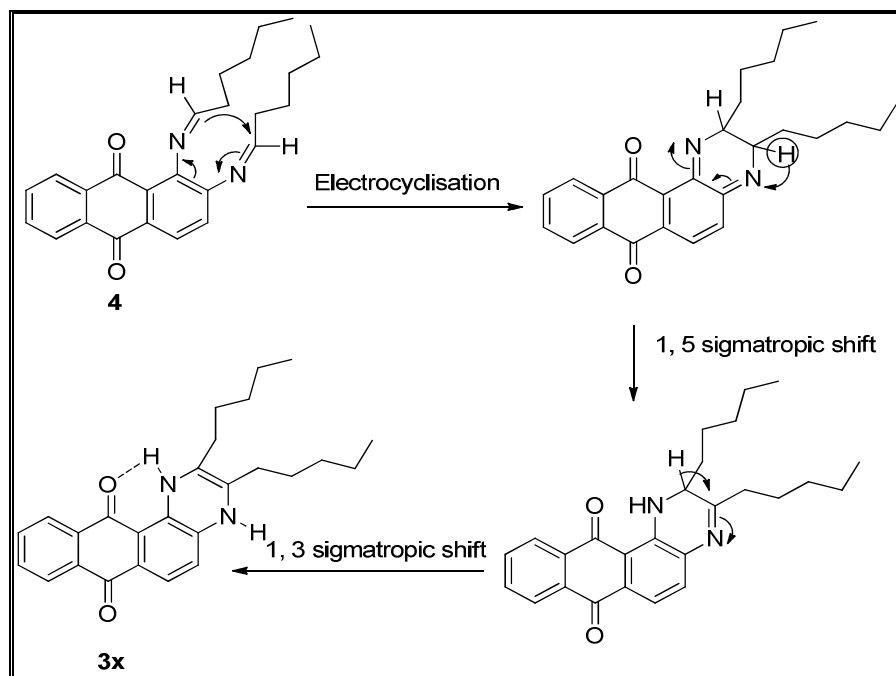
**1** as discussed earlier. Both of the amino groups would now be available on the catalyst surface to react in tandem with aldehyde group in presence of PTA. At this stage it became imperative to understand the oxidation step of this CCO reaction which was carried out under aerobic condition. To investigate the role of aerial oxygen, if any, we repeated the experiment under dry nitrogen atmosphere when an altogether different reaction pathway was identified after the isolation of a novel compound, 2,3-dipentyl-naphtho[2,3-*f*]quinoxaline-7,12(1*H*,4*H*)-dione, **3x** along with unreacted 1,2-diaminoanthraquinone **1** approximately in the ratio of 1:2 (**Scheme 2**).



**Scheme 2.** 1,2-diaminoanthraquinone **1** reacts with hexanal **2o** in presence of PTA under nitrogen atmosphere forming **3x**

A plausible mechanistic pathway was presented (**Scheme 3**) to explain the formation of **3x** under oxygen-free condition. Initially 1,2-diaminoanthraquinone **1** would form the diimine derivative **4** with hexanal **2o** followed by a cascade pathway involving 6 $\pi$  electrocycisation and two consecutive 1,5- and 1,3-prototropic shifts to produce **3x**. Aromatization of the compound **3x** did not occur in absence of oxidative environment probably due to the formation of intramolecular hydrogen bond between N-H proton and the C-11 carbonyl group of the quinone ring which was reflected in the  $^1\text{H-NMR}$  spectrum of **3x**. A broad singlet at  $\delta$  11.04 was assigned to H-bonded -NH- whereas the singlet at  $\delta$  6.89 was attributed to free -NH- function. This type of

$6\pi$  electrocyclisation of diimine derived from aromatic 1,2-diamine and aldehyde in inert atmosphere was not reported earlier in the literature.



**Scheme 3.** A plausible mechanistic pathway to the formation of **3x**

Therefore from the above study it may be concluded that the aerial oxygen was required for oxidative dehydrogenation of the dihydroimidazole intermediate leading to the formation of heteroaromatic imidazole moiety and/or regeneration of PTA as oxidant from low valence states of tungsten.<sup>16e</sup>

A study regarding recycling of PTA was also performed and it was successfully reused four times without any pretreatment. To verify the property of reused PTA, field emission scanning electron microscopy (FESEM) images of fresh and reused PTA (after first cycle) was taken which indicated no obvious change in the morphology of the catalyst (see **ESI, Fig. S1**).

The intrinsic non-covalent interactions of low molecular mass self-aggregated organic materials (LMSOM) are identifiable from its stacking pattern in the crystal lattice.<sup>4b, 28, 29</sup> We could obtain a single crystal of the compound **3t** (**Fig. 2**) (more information see **ESI**).

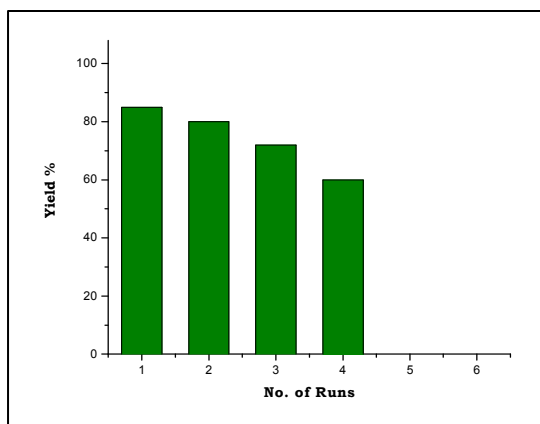


**Fig 1:** Reusability graph of PTA

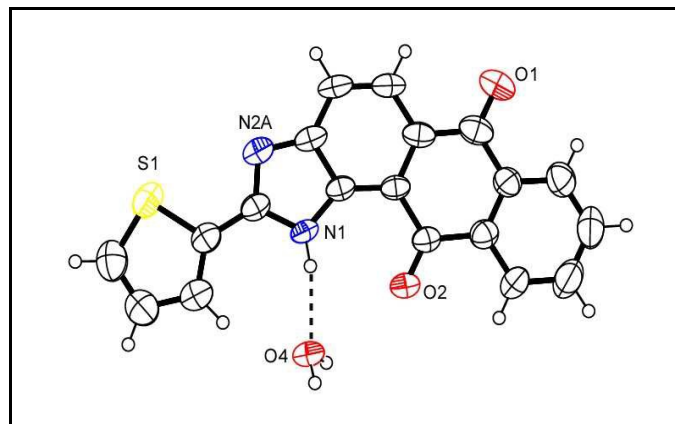


**Fig 2:** X-ray crystallographic structure of compound **3t**

To investigate the effect of the crystal structure on molecular aggregation, we had performed analysis of the X-ray data of **3t** using SHELXS 97,<sup>30</sup> SHELXL 97,<sup>31</sup> PLATON 99,<sup>32</sup> ORTEP-32<sup>33</sup> and WINGX system ver-1.64.<sup>34</sup> (**Fig. 3a-d**). It has been observed from the analysis that several types of intermolecular hydrogen bonding interactions (**Fig. 3a and 3b**) are present in the crystal lattice of **3t** (see **ESI**, **Table-S2**). Besides these intermolecular H-bonding interactions, an inter-molecular  $\pi$ - $\pi$  stacking interaction is also present between two phenyl rings of anthraquinone unit of the two neighboring molecules with a centroid Cg...Cg distance of 3.596(4) Å to generate a 1D chain (**Fig. 3c**) along the crystallographic 'c' axis. Both H-bonding and  $\pi$ - $\pi$  stacking interactions present in the crystal lattice of **3t** formed a 3D network (**Fig. 3d**) with a brickwork type arrangement containing a knot of water molecule. A bent and head-to-tail

array of the molecules in the crystal lattice indicated the J-aggregation property of the compound.<sup>4b</sup>

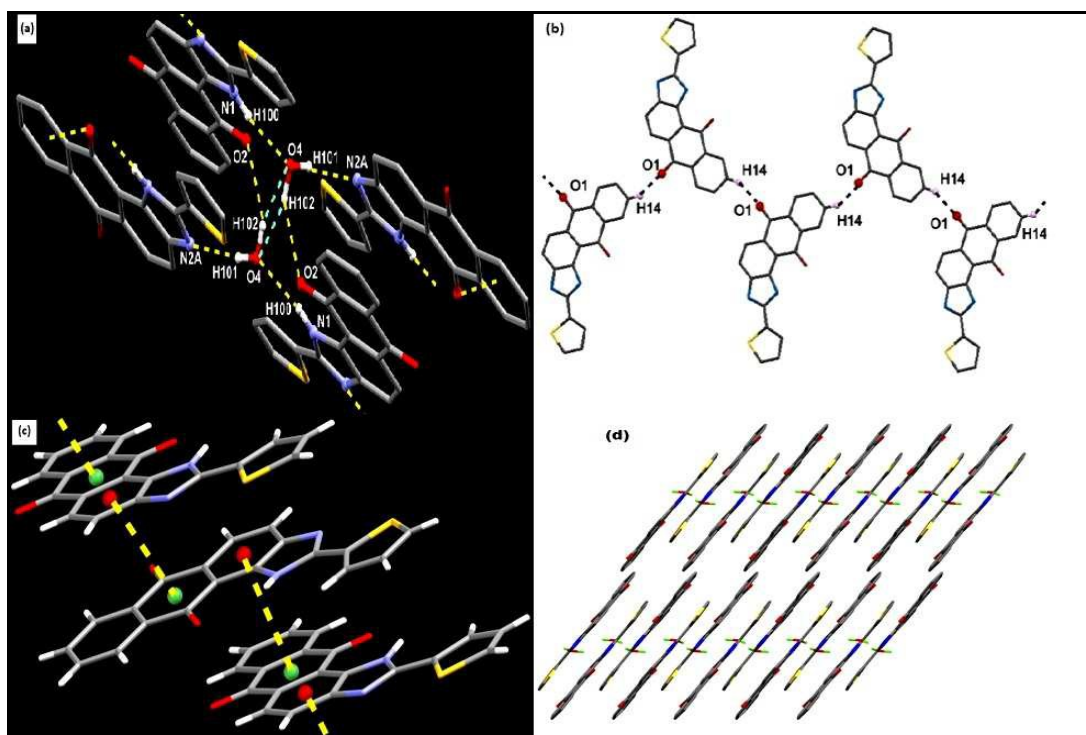


**Figure 3:** (a) Hydrogen bonding pattern between water molecule and anthraimidazoledione moiety; (b) H-bonding between carbonyl oxygen and the aromatic hydrogen atom of neighboring molecule; (c) Intermolecular  $\pi$ - $\pi$  stacking between the two phenyl rings of neighboring molecule; (d) The 3D network of compound **3t** having brickwork-like arrangement with a water molecule like a knot.

A powder XRD study was performed for **3t** by using X-ray diffraction (XRD) analysis applying Sherrer's formula  $D_p \propto 0.9411/b \cos \theta$ ; where X-ray wave length ( $\lambda$ )  $\propto 1.5406 \text{ \AA}$ ,  $\theta$   $\propto$  Bragg's diffraction angle for the planes (010), (110), (111), (200), (211), (220), (311), (222) and (440) and  $b$  as the corresponding full width at half maximum (FWHM) value<sup>35</sup> A comparison between the simulated PXRD derived from single crystal diffraction data of **3t** with the experimental one clearly showed that it was pure and entirely crystalline in the bulk state (see ESI, Fig. S2). Similar comparative PXRD studies between **3t** and **3p** (see ESI, Fig. S3) using

the planes (010), (110), (111), (200), (210) and (310) for **3p** also demonstrated the existence of micro-crystallinity of **3p** in its bulk state.<sup>35, 36</sup>

It is relevant to mention here that **3p** and **3t** varies in their substituent pattern at 2-position of the imidazole ring with a thiophene ring for the former and a long aliphatic chain of ten carbon atoms for the latter. Non-covalent interactions observed in the crystal lattice of **3t** and the micro-crystalline nature of both **3p** and **3t** as evinced from their respective PXRD data prompted us to Scanning Electron Microscopy (SEM) study. Compound **3t** in toluene formed well-defined bundles of needle-shaped nanowires (width 129 nm) with a knot (**Fig. 4a** and **4b**), whereas **3p** spontaneously aggregates as ordered hemispherical particle assemblies with several holes on the surface ranging from 148-410 nm (**Fig. 4c** and **4d**) in toluene. Presence of several hydrogen bonding and  $\pi$ - $\pi$  stacking interactions within the framework of the  $\pi$ -extended planar molecule **3t** would be the main driving force for the formation of the aforesaid morphology. On the other hand, molecule **3p** assumes a unique amphiphilic nature bearing a polar head (anthraimidazoledione part) and an elongated flexible hydrophobic tail (ten carbon alkyl chain) which might compel the molecule to aggregate as an ordered particle assembly with holes on the surface.<sup>37</sup> Thus in case of **3p**, morphology is dominated by the van der Waals interactions involving the alkyl chains.<sup>37, 38</sup>

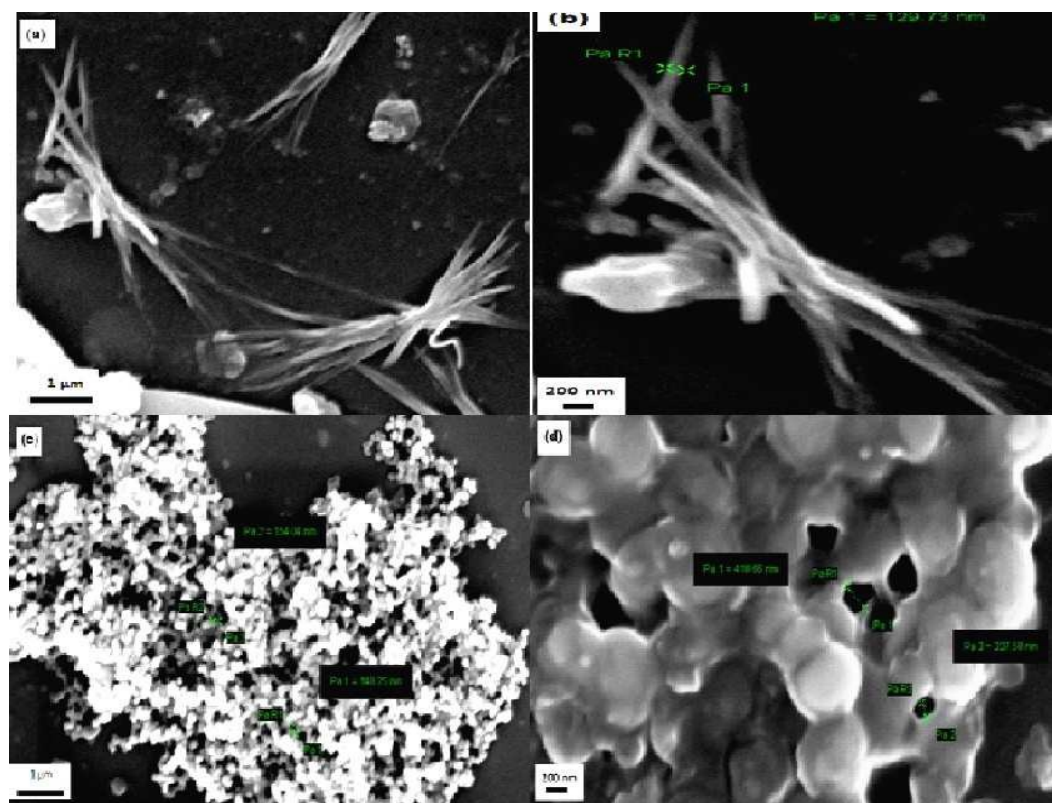


**Figure 4:** (a) and (b) SEM images of compound **3t** showing bundle of needle-shaped nanowire with a knot; scale bar represent 1  $\mu\text{m}$  and 200 nm respectively; (c) and (d) SEM images of compound **3p** showing an ordered hemispherical particle assembly with several holes on surface; scale bar represents 1  $\mu\text{m}$  and 200 nm respectively)

As LMSOMs exhibit unique optical and optoelectronic properties both in their solid and solution state<sup>28</sup> we took UV-Vis absorption spectra of the representative compounds ( $1 \times 10^{-6}$  M) in polar aprotic and non-polar solvents and in the solid state (**Fig. 5**). In case of **3p**, a  $\pi-\pi^*$  transition band of the aromatic ring appears at  $\sim 390$  nm in toluene ( $1 \times 10^{-6}$  M) and it shows slight solvent dependency in acetonitrile solvent ( $\lambda_{\text{max}} = \sim 380$  nm,  $1 \times 10^{-6}$  M). The absorption spectrum of **3p** in the solid state is found to be comparatively broad and flat at the peak position (**Fig. 5a**) may be due to the self-aggregation in the solid state.<sup>39</sup> The same

$\pi-\pi^*$  transition of **3t** (421 nm in toluene and 417 nm in acetonitrile, both concentrations are  $1 \times 10^{-6}$  M) exhibited red shift due to extended conjugation (**Fig. 5b**). Here also absorption band in solid is broad and flat at the peak position (J-aggregation as per X-ray study). Systematic concentration dependant UV-VIS spectroscopy experiments for both **3p** and **3t** revealed that with increase in concentrations (from  $10^{-6}$  to  $10^{-4}$  M), the peak saturated at the OD value which were almost equivalent to the spectra obtained in their solid state.

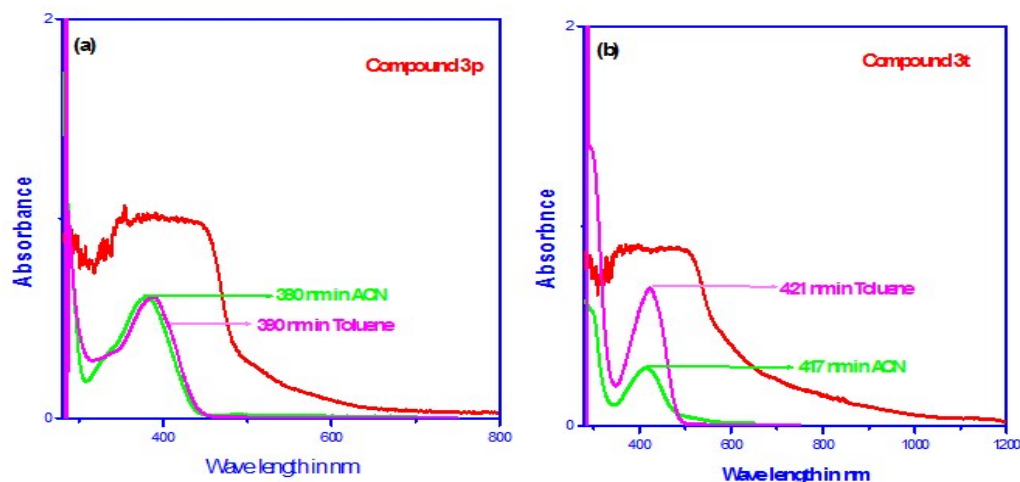


**Figure 5:** (a) Comparison of UV-Vis spectra of the compound **3p** in solution ( $1 \times 10^{-6}$  M) and solid phase.

(b) Comparison of UV-Vis spectra of the compound **3t** in solution ( $1 \times 10^{-6}$  M) and solid phase.

However **3p** and **3t** showed contrasting behavior in their emission spectroscopy. Compound **3t** exhibited emission maxima at 527 nm ( $\lambda_{\text{ex}} = 421$  nm) in toluene solution ( $1 \times 10^{-6}$  M) and showed higher solvent dependency (557 nm in ACN solvent,  $\lambda_{\text{ex}} = 417$  nm,  $1 \times 10^{-6}$  M).

**Fig. 6a).** In solid form, it furnished slightly different spectral pattern with peak at 607 nm (irradiated at  $\sim 502$  nm) having higher fluorescence intensity (**Fig. 6b**). In comparison, compound **3p** was found to be non-emissive in acetonitrile ( $\lambda_{\text{ex}} = 380$  nm) as well as in toluene solution ( $\lambda_{\text{ex}} = 390$  nm) (both concentrations are  $1 \times 10^{-6}$  M), but showed high fluorescence intensity (nearly 400 times) in the aggregated solid state ( $\lambda_{\text{em}} = 530$  nm, irradiated at  $\sim 439$  nm) as indicated in **Fig. 6a**. Presence of long tail with high flexibility may be the cause of non-emission property of **3p** in solution ( $1 \times 10^{-6}$  M) as flexible bonds usually open up non-radiative channels.

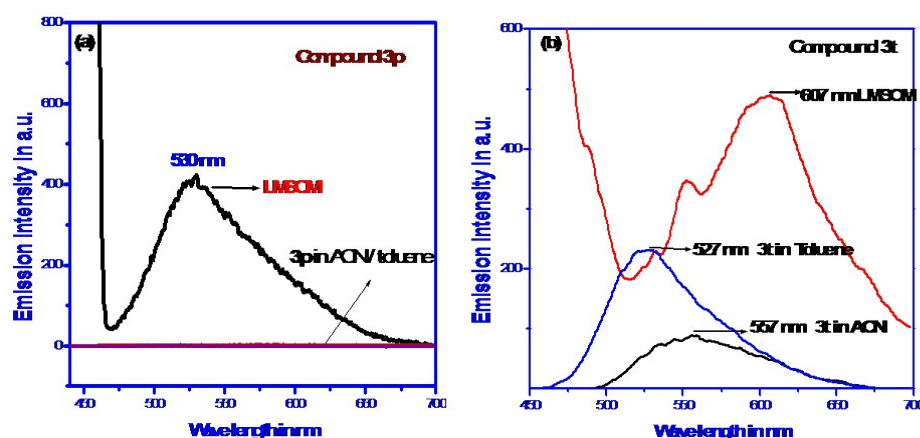


**Figure 6:**(a) Comparison of fluorescence spectra of the compound **3p** in acetonitrile ( $\lambda_{\text{ex}} = 380$  nm,  $1 \times 10^{-6}$  M) and toluene solution ( $\lambda_{\text{ex}} = 390$  nm,  $1 \times 10^{-6}$  M) and solid phase ( $\lambda_{\text{ex}} = 439$  nm). (b) Comparison of fluorescence spectra of the compound **3t** in ACN ( $\lambda_{\text{ex}} = 417$  nm,  $1 \times 10^{-6}$  M) and in toluene solution ( $\lambda_{\text{ex}} = 421$  nm,  $1 \times 10^{-6}$  M) and solid phase ( $\lambda_{\text{ex}} = 502$  nm).

Citations of some particular organic entities having enhanced emission in their solid state are correlated with the intra- and intermolecular forces present in the molecules.<sup>39</sup> Intra-molecular effects like conformational aspects of the chromophore influence the radiation process in solid state or in solution phase.<sup>40</sup> Inter-molecular interactions such as molecular aggregation (H-type or J-type) are reported to control the fluorescence efficiency of the molecule.<sup>41</sup> Generally

J-aggregated molecules showed comparatively higher fluorescence intensity due to their bent or head-to-tail arrangement with a red shift in UV absorption maxima.<sup>41</sup> But the unusual strong fluorescence efficiency of the compound **3p** in J-aggregated form compared to non-emissive nature of its acetonitrile or toluene solution can be explained in terms of non-radiative channels operated through flexible bonds. In **3p**, intermolecular forces cause aggregation induced rigidity resulting in high solid-state emission. But in solution, both in polar or non-polar medium, conformational aspects of the long flexible aliphatic chain is dominating, thus favoring energy dissipative paths and it becomes non-emissive. As a consequence, **3p** imparts a fluorescence “ON-OFF” mechanism from solid to solution state. In case of **3t**, structural flexibility is less and it shows emission in the solution phase and enhances its emission intensity in the solid by the formation of J-aggregated state.

The results obtained from emission spectrum prompted us to carry out DFT calculations for **3p** and **3t**. The HOMO-LUMO pictures obtained by using B3LYP/6-311++G as the functional and basis set showed that HOMOs for both molecules are localized on their respective substituent arms whereas the LUMOs are contributed by the anthraquinone units (see ESI, Fig. S4). For this reason, photophysical properties of these molecules would be guided by the nature of the substituent present at the 2-position of the imidazole ring as observed in this case.<sup>42</sup>

Considering all the morphological and photophysical phenomena we may anticipate that anthraimidazolediones containing a lipophilic long aliphatic chain and polar anthraquinone moiety could find application in the field of organogelators.<sup>37</sup> Furthermore, the holes present in the SEM structure of **3p** are very unusual which might find use as a receptor site or host or a transporter.<sup>43</sup> Both **3p** and **3t**, due to their remarkable fluorescent nature, are eligible candidates for application as chemical sensors.

## Conclusions

In conclusion, a straightforward tandem green protocol was developed for the chemoselective synthesis of anthra[1,2-*d*]imidazole-6,11-dione derivatives via CCO reaction employing PTA as reusable catalyst on PEG-400 support in open air. In inert atmosphere, methodology adopted a complete different pathway leading to the formation of unique naphthoquinoxaline derivative. Wide range of applicability of the reaction procedure was proved by using an array of aldehydes which furnish good to excellent yields of the anthraimidazoledione derivatives. Single crystal data of compound **3t** reveals distinct crystal packing pattern with  $\pi$ - $\pi$  stacking and hydrogen bonding interactions. **3p** and **3t**, bearing different substituents at 2-position of the anthra [1,2-*d*]imidazole-6,11-dione moieties, showed micro-crystalline nature in bulk state from PXRD studies and different morphologies in their corresponding SEM images which justified the effect of substituents. DFT studies of aforesaid compounds revealed similarities in their HOMO-LUMO characteristics. Both molecules show comparable J-aggregation behavior and form LMSOMs in their solid state as evidenced from photophysical studies. Further studies related to the generation of novel nanomaterials based on this scaffold possessing interesting optoelectronic and gelation properties and also as chemosensing agents are in progress in our laboratory.

## Experimental

### General reaction procedure for the formation of anthra [1,2-*d*]imidazole-6,11-diones (**3a-w**):

A mixture of 1,2-diaminoanthraquinone **1** (1 mmol), aldehydes **2** (1 mmol) were stirred at 80°C in an oil bath in 3 mL PEG-400 support in open air. To this stirring mixture, phosphotungstic acid (10 mol %) was added and stirred for stipulated time. After completion (as monitored by

TLC), the reaction mixture was cooled to 0-5°C and extracted with ethyl acetate. The reaction mixture was filtered and the filtered out solid PTA was washed with acetone and dried under vacuum for reuse. Ethyl acetate part was washed with water thrice to remove PEG-400 and evaporated under vacuum. Pure product was isolated by column chromatography over silica gel using different mixtures of petroleum ether: ethyl acetate.

Known products were compared with their m.p. and spectral data as obtained from concerned literature. Spectral data of representative compounds, **3p** and **3t** are listed below;

**(±)2-(2,6-dimethylhept-5-enyl)-1H-anthra[1,2-d]imidazole-6,11-dione (3p).** Yield: 242 mg, 90%, yellow crystalline solid; Mp 149-150°C; <sup>1</sup>H NMR (300 MHz, DMSO-d<sub>6</sub>) δ 12.94 (s, 1H), 8.09-8.05 (m, 2H), 7.88 (s, 2H), 7.80-7.77 (m, 2H), ca. 4.96 (m, 1H), 2.85-2.83 (m, 1H), 2.74-2.71 (m, 1H), 2.10-1.89 (m, 2H), 1.51 (s, 3H), 1.44 (s, 3H), 1.35-1.23 (m, 1H), 1.20-1.09 (m, 2H), 0.81(d, *J* = 6.6 Hz, 3H); <sup>13</sup>C NMR (75 MHz, DMSO-d<sub>6</sub>) δ 183.8, 182.9, 162.3, 149.7, 134.8, 134.6, 133.6, 133.4, 132.3, 131.1, 127.6, 127.2, 126.6, 124.9, 124.7, 120.6, 118.3, 36.9, 35.9, 32.6, 25.9, 25.4, 19.8, 17.9; IR ν<sub>max</sub> (KBr) cm<sup>-1</sup> 3737, 3359, 2927, 2365, 1655, 1579, 1509; anal. calcd for C<sub>24</sub>H<sub>24</sub>N<sub>2</sub>O<sub>2</sub>: C: 77.39, H: 6.49, N: 7.52 %, found: C: 77.37, H: 6.50, N: 7.50 %.

**2-(thiophen-2-yl)-1H-anthra[1,2-d]imidazole-6,11-dione (3t).** Yield: 280 mg, 92%, brown crystalline solid; Mp 282-283°C; <sup>1</sup>H NMR (300 MHz, DMSO-d<sub>6</sub>) δ 13.40 (s, 1H), 8.51 (d, *J* = 3 Hz, 1H), 8.21-8.16 (m, 2H), 8.03 (s, 2H), 7.91-7.89 (m, 2H), 7.83-7.82 (m, 1H), 7.26-7.25 (m, 1H); <sup>13</sup>C NMR (75 MHz, DMSO-d<sub>6</sub>) δ 183.7, 182.8, 153.6, 149.7, 134.9, 134.7, 133.6, 133.2, 132.8, 132.1, 131.5, 130.9, 129.2, 128.4, 127.3, 126.7, 124.9, 121.7, 118.9; IR ν<sub>max</sub> (KBr) cm<sup>-1</sup> 3539, 3390, 3075, 2925, 1655, 1577, 1560; anal. calcd for C<sub>19</sub>H<sub>10</sub>N<sub>2</sub>O<sub>2</sub>S: C: 69.08, H: 3.05, N: 8.48 %, found: C: 69.06, H: 3.06, N: 8.45 %.

### General reaction procedure for synthesis of 2,3-dipentynaphtho[2,3-*f*]quinoxaline-7,12(1*H*,4*H*)-dione (3x):

A mixture of 1,2-diaminoanthraquinone **1** (1 mmol), aldehyde **2o** (1.2 mmol) were stirred at 80 °C in an oil bath in 3 mL PEG-400 support under N<sub>2</sub>-atmosphere. To this stirring mixture phosphotungstic acid (10 mol %) was added and stirred for one hour. Then the reaction mixture was cooled to 0-5 °C and extracted with ethyl acetate. Ethyl acetate part was washed with water thrice to remove PEG-400 and evaporated under vacuum. Pure product was isolated by column chromatography over silica gel using different mixtures of petroleum ether:ethyl acetate.

**2,3-dipentynaphtho[2,3-*f*]quinoxaline-7,12(1*H*,4*H*)-dione (3x).** Yield: 150 mg, 37%, yellow crystalline solid; Mp 124-126 °C; <sup>1</sup>H NMR (300 MHz, CDCl<sub>3</sub>) δ 11.04 (br. s, 1H), 8.28-8.18 (m, 4H), 7.77-7.45 (m, 2H), 6.89 (br. s, 1H), ca. 2.69 (m, 2H), ca. 2.35 (m, 2H), 1.50-1.32 (m, 12H), 0.90-0.86 (m, 6H); <sup>13</sup>C NMR (75 MHz, CDCl<sub>3</sub>) δ 185.1, 182.2, 157.4, 134.8, 134.5, 134.0, 133.9, 133.0, 131.5, 129.1, 127.8, 126.6, 124.3, 122.9, 118.0, 31.7, 31.5, 29.1, 28.7, 27.7, 22.7, 22.5, 13.9; IR ν<sub>max</sub> (KBr) cm<sup>-1</sup> 3326, 2925, 2854, 1660, 1583, 1519; anal. calcd for C<sub>26</sub>H<sub>30</sub>N<sub>2</sub>O<sub>2</sub>: C: 77.58, H: 7.51, N: 6.96 %, found: C: 77.56, H: 7.50, N: 6.94 %. HRMS (TOF MS ES<sup>+</sup>): *m/z* calcd for (M-H)<sup>+</sup> C<sub>26</sub>H<sub>30</sub>N<sub>2</sub>O<sub>2</sub>- 403.2385; found 403.2339.

### Acknowledgements

We gratefully acknowledge the financial support received from the University of Calcutta. Crystallography was performed at the DST-FIST, India-funded Single Crystal Diffractometer facility at the Department of Chemistry, University of Calcutta. We would like to thank the Centre for Research in Nanoscience and Nanotechnology, University of Calcutta for providing SEM and FESEM facilities. We express our gratitude to Lakshmi Kanta Das and Aniruddha

Ganguly for their valuable suggestions. We further express our gratefulness to Dr. Dipankar Chakraborty for providing powder XRD facilities.

## References

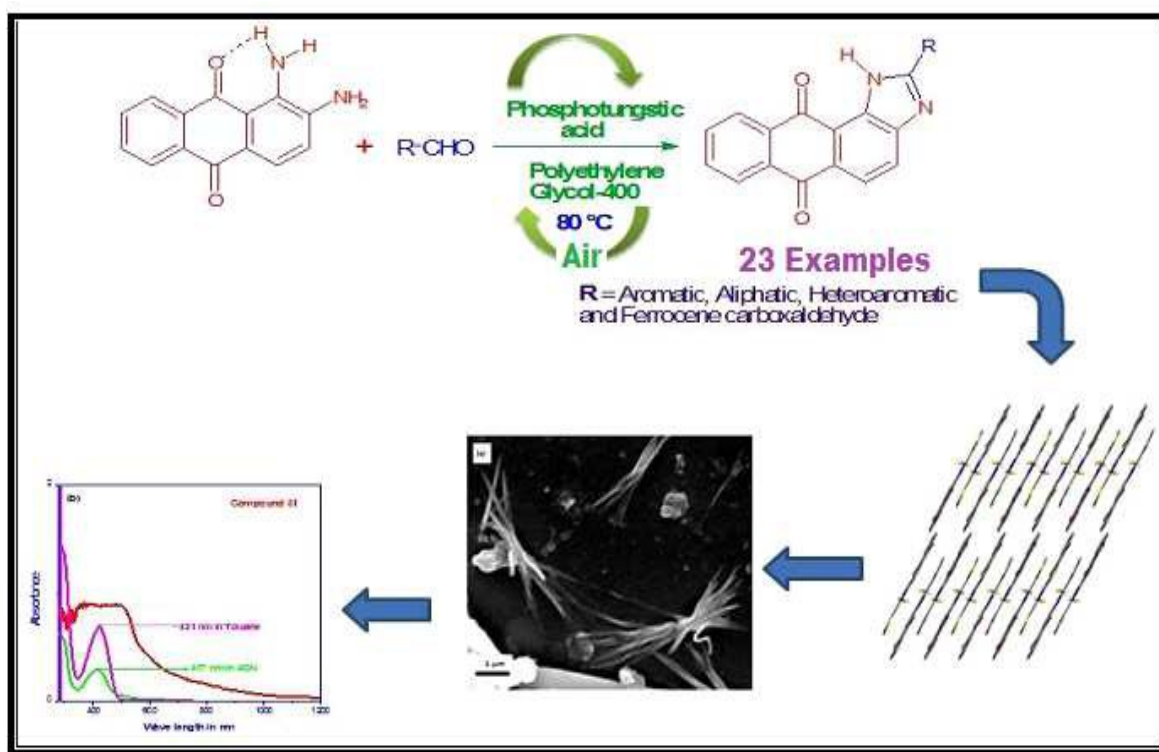
1. (a) M.-B. Madec, D. Crouch, G. Llorente, T. J. Whittle, M. Geoghegan and S. G. Yeates, *J. Mater. Chem.*, 2008, **18**, 3230; (b) T.-T. Bui and F. Goubard, *EPJ Photovoltaics*, 2013, **4**, 40402; (c) V. Coropceanu, H. Li, P. Winget, L. Zhu and J.-L. Brédas, *Annu. Rev. Mater. Res.*, 2013, **43**, 63.
2. (a) C. Reese and Z. Bao, *Materials Today*, 2007, **10**, 20; (b) C. D. Dimitrakopoulos and D. J. Masearo, *IBM J. RES. & DEV.*, 2001, **45**, 11; (c) A. Facchetti, *Materials Today*, 2007, **10**, 28.
3. D. Volz, M. Wallesch, C. Fléchon, M. Danz, A. Verma, J. M. Navarro, D. M. Zink, S. Bräse and T. Baumann, *Green Chem.*, 2015, **17**, 1988.
4. (a) T. W. Bell and N. M. Hext, *Chem. Soc. Rev.*, 2004, **33**, 589; (b) Y. S. Zhao, H. Fu, A. Peng, Y. Ma, D. Xiao and J. Yao, *Adv. Mater.*, 2008, **20**, 2859; (c) M. Mille, J.-F. Lame`re, F. Rodrigues and S. Fery-Forgues, *Langmuir*, 2008, **24**, 2671.
5. (a) Q. H. Cui, Y. S. Zhao and J. Yao, *Adv. Mater.*, 2014, **26**, 6852; (b) M.-S. Schiedel, C. A. Briehn and P. Bäuerle, *Angew. Chem., Int. Ed.*, 2001, **40**, 4677.
6. (a) L. Zang, Y. Che and J. S. Moore, *Acc. Chem. Res.*, 2008, **41**, 1596; (b) Y. S. Zhao, W. Yang, D. Xiao, X. Sheng, X. Yang, Z. Shuai, Y. Luo and J. Yao, *Chem. Mater.*, 2005, **17**, 6430.
7. D. K. Maiti, S. Halder,; P. Pandit, N. Chatterjee, D. De Joarder, N. Pramanik, Y. Saima, A. Patra and P. K. Maiti, *J. Org. Chem.*, 2009, **74**, 8086.

8. S. S. Panda, R. Malik and S. C. Jain, *Current Organic Chemistry*, 2012, **16**, 1905.
9. S. Saha, A. Ghosh, P. Mahato, S. Mishra, S. K. Mishra, E. Suresh, S. Das and A. Das, *Org. Lett.*, 2010, **12**, 3406.
10. S. M. Sondhi, J. Singh, P. Roy, S. K. Agrawal and A. K. Saxena, *Med. Chem. Res.*, 2011, **20**, 887.
11. (a) E. N. da Silva Jr., B. C. Cavalcanti, T. T. Guimarães, M. do C. F.R. Pinto, I. O. Cabral, C. Pessoa, L. V. Costa-Lotufo, M. O. de Moraes, C. K. Z. de Andrade, M. R. dos Santos, C. A. de Simone, M. O. F. Goulart and A. V. Pinto, *Eur. J. Med. Chem.*, 2011, **46**, 399; (b) Y. Ooyama, T. Nakamura and K. Yoshida, *New. J. Chem.*, 2005, **29**, 447.
12. N. Kumari, S. Jha and S. Bhattacharya, *J. Org. Chem.*, 2011, **76**, 8215.
13. V. Luxami and S. Kumar, *Dalton Trans.*, 2012, **41**, 4588.
14. (a) R. M. F. Batista, E. Oliveira, S. P. G. Costa, C. Lodeiro and M. M. M. Raposo, *Org. Lett.*, 2007, **9**, 3201; (b) R. M. F. Batista, S. P. G. Costa and M. M. M. Raposo, *J. Photochem. Photobiol A: Chemistry*, 2013, **259**, 33; (c) R. M. F. Batista, E. Oliveira, S. P. G. Costa, C. Lodeiro and M. M. M. Raposo, *Supramolecular Chemistry*, 2014, **26**, 71; (d) R. M. F. Batista, S. P. G. Costa and M. M. M. Raposo, *Sensors and Actuators B*, 2014, **191**, 791.
15. H.-S. Huang, T.-C. Chen, R.-H. Chen, K.-F. Huang, F.-C. Huang, J.-R. Jhan, C.-L. Chen, C.-C. Lee, Y. Lo and J.-J. Lin, *Bioorg. Med. Chem.*, 2009, **17**, 7418.
16. (a) G. Li, Y. Ding, J. Wang, X. Wang and J. Suo, *J. Mol. Catal. A*, 2007, **262**, 67; (b) A. Haimov and R. Neumann, *Chem. Commun.*, 2002, 876; (c) D. C. Duncan and C. L. Hill, *J. Am. Chem. Soc.*, 1997, **119**, 243; (d) R. Neumann and M. Levin, *J. Am. Chem. Soc.*, 1992,

- 114**, 7278; (e) A. Hiskia and E. Papaconstantinou, *Inorg. Chem.*, 1992, **31**, 167; (f) R. Neumann and M. Levin, *J. Org. Chem.*, 1991, **56**, 5707.
17. (a) S.-S. Wang and G.-Y. Yang, *Chem. Rev.*, 2015, **115**, 4893; (b) Y. Zhou,; G. Chen, Z. Long and J. Wang, *RSC Adv.*, 2014, **4**, 42092; (c) M. Misono, I. Ono, G. Koyano and A. Aoshima, *Pure Appl. Chem.*, 2000, **72**, 1305.
18. M. Dabiri and S. Bashribod, *Molecules*, 2009, **14**, 1126.
19. R. S. Keri and K. M. Hosamani, *Catal. Lett.*, 2009, **131**, 321.
20. K. Vanlaldinpuia and G. Bez, *Tet. Lett.*, 2011, **52**, 3759.
21. K. C. S. Achar, K. M. Hosamani and H. R. Seetharamareddy, *Synth. Commun.*, 2011, **41**, 33.
22. I. V. Kozhevnikov, *J. Mol. Catal. A*, 2009, **305**, 104.
23. N. Mizuno and M. Misono, *Chem. Rev.*, 1998, **98**, 199.
24. E. Colacino, J. Martinez, F. Lamaty, L. S. Patrikeeva, L. L. Khemchyan, V. P. Ananikov and I. P. Beletskaya, *Coord. Chem. Rev.*, 2012, **256**, 2893.
25. J. Chen, S. K. Spear, J. G. Huddleston and R. D. Rogers, *Green. Chem.*, 2005, **7**, 64.
26. K. Bahrami, M. M. Khodaei and A. Nejati, *Green. Chem.*, 2010, **12**, 1237.
27. B. Bhattacharyya and K. P. Dhara, *J. Indian Chem. Soc.*, 2013, **90**, 1749.
28. Y. Yan and Y. S. Zhao, *Chem. Soc. Rev.*, 2014, **43**, 4325.
29. L. J. Prins, D. N. Reinhoudt and P. Timmerman, *Angew. Chem., Int. Ed.*, 2001, **40**, 2382.
30. G. M. Sheldrick, *SHELXS 97, Program for Structure Solution*, University of Göttingen, Germany, 1997.
31. G. M. Sheldrick, *SHELXL 97, Program for Crystal Structure Refinement*, University of Göttingen, Germany, 1997.

32. A. L. Spek, PLATON. Molecular Geometry Program. *J. Appl. Crystallogr.*, 2003, **36**, 7.
33. L. J. Farrugia, *J. Appl. Crystallogr.*, 1997, **30**, 565.
34. L. J. Farrugia, *J. Appl. Crystallogr.*, 1999, **32**, 837.
35. Y. Waseda, E. Matsubara and K. Shinoda, *X-Ray Diffraction Crystallography Introduction, Examples and Solved Problems*, Springer-Verlag Berlin Heidelberg, 2011.
36. Y. Wang, H. Fu, A. Peng, Y. Zhao, J. Ma, Y. Ma and J. Yao, *Chem. Commun.*, 2007, 1623.
37. X. Shen, T. Jiao, Q. Zhang, H. Guo, Y. Lv, J. Zhou and F. Gao, *J. Nanomater.*, 2013, DOI:10.1155/2013/409087.
38. T. Jiao, Q. Huang, Q. Zhang, D. Xiao, J. Zhou and F. Gao, *Nanoscale Research Letters*, 2013, **8**, 278.
39. B.-K. An, S.-K. Kwon, S.-D. Jung and S. Y. Park, *J. Am. Chem. Soc.*, 2002, **124**, 14410.
40. M. M. Souza, G. Rumbles, I. R. Gould, H. Amer, I. D. W. Samuel, S. C. Moratti and A. B. Holmes, *Synth. Met.*, 2000, **111**, 539.
41. W. I. Gruszecki, *J. Biol. Phys.*, 1991, **18**, 99.
42. (a) Y. Yang, H. Wang, F. Liu, D. Yang, S. Bo, L. Qui, Z. Zhen and X. Liu, *Phys. Chem. Chem. Phys.*, 2015, **17**, 5776; (b) G.-Y. Li, G.-J. Zhao, Y.-H. Liu, K.-L. Han and G.-Z. He, *J. Comput. Chem.*, 2010, **31**, 1759.
43. T.-T. Bui and F. Goubard, *EPJ Photovoltaics*, 2013, **4**, 40402.
44. X. J. Peng, Y. K. Wu, J. L. Fan, M. Z. Tian and K.-L. Han, *J. Org. Chem.*, 2005, **170**, 10524.

## Graphical Abstract



One-pot protocol for structurally tailored J-aggregated anthra[1,2-*d*]imidazole-6,11-dione was developed via tandem cyclocondensation *cum* oxidation, catalyzed by heterogeneous, reusable phosphotungstic acid in PEG-400 support in presence of air. Photophysical studies confirm their strong J-aggregation properties while they exhibit contrasting fluorescence behaviors during transition from solution to nanostructured solid state.